J. Chem. Sci. (2021) 133:100
https://doi.org/10.1007/s12039-021-01964-9

REGULAR ARTICLE

Special Issue on Beyond Classical Chemistry

Adsorption of gases on small–pore aluminum bisphosphonate MOF MIL–91(Al)

PRUDHVIRAJ MEDIKONDA[a], RAJSEKHAR PILLI[a], CHIVUKULA V SASTRI[b] and SASIDHAR GUMMA[c,*]

[a]Department of Chemical Engineering, Indian Institute of Technology Guwahati, Guwahati 781039, India
[b]Department of Chemistry, Indian Institute of Technology Guwahati, Guwahati 781039, India
[c]Department of Chemical Engineering, Indian Institute of Technology Tirupati, Tirupati 517506, India
E-mail: s.gumma@iittp.ac.in

MS received 5 July 2021; revised 19 July 2021; accepted 28 July 2021

Abstract. In this work, the adsorption isotherms of small pore bisphosphonate MOF MIL–91(Al) was evaluated for permanent gases *viz.*, CO_2, CO, N_2, CH_4, C_2H_6 and C_3H_8. Gravimetric adsorption measurements were performed at three different temperatures 294, 318, 358 K and a wide range of pressures. For all measured gases type–1 adsorption isotherm was observed. Isotherms were modeled using the Virial equation and calculated fit parameters were used to calculate the enthalpy of adsorption. CO_2 exhibits moderate enthalpy of adsorption along with excellent selectivity on MIL–91 (Al), thereby making it an attractive adsorbent for gas separation applications.

Keywords. MIL–91(Al); Small pore MOF; Gas adsorption; CO_2 selectivity; Ideal adsorbed solution theory.

1. Introduction

Metal-organic frameworks (MOFs) are a new class of crystalline microporous materials that have been widely used for applications of gas storage, separation, sensing and catalysis.[1–10] Due to the wide variety of organic linkers and metal centers, a distinct characteristic of MOF can be synthesized.[11] In spite of attractive properties, some MOFs have exhibited poor thermal and chemical stability. MOF MIL–91 (Al) is made up of phosphonate ligand and has pores with an opening of 3.5 Å. This may be a potential candidate for targeted applications such as selective capture of CO_2 from other gases with a larger kinetic diameter.[12]

A small pore bisphosphonate MOF MIL–91(Al) is one of the few porous phosphonate MOFs reported in the literature. It exhibits strong interaction of CO_2 due to the presence of phosphonate P–OH and N–H functional groups and confined pore size make them more selective.[12] MIL–91 (Al) is formed from corner-sharing of $Al(OH)_2O_4$ and protonated bisphosphonate linker (Figure 1) giving rise to a three-dimensional porous structure.[13] In this arrangement, the organic ligand links neighbouring Al–OH–Al chains leaving channels of 3.5×3.5 Å along *b*–axis (there is no significant porosity along *a*–axis and *c*–axis), which makes this MOF suitable for targeted *sieving* applications in gas separations. In this work, we report the equilibrium adsorption isotherms of industrially relevant gases *viz.,* CO_2, CO, N_2, CH_4, C_2H_6 and C_3H_8 on this MOF at three different temperatures and over a wide range of pressure. Adsorption enthalpy was calculated from isotherm models and Ideal Adsorbed Solution Theory (IAST) was used to predict the selectivity in binary mixtures.

2. Experimental

2.1 *Material synthesis and characterization*

MIL–91(Al) was synthesized as per the procedure reported in Serre *et al.* [13] Details were given in supporting information. The Brunauer–Emmett–Teller

*For correspondence

Supplementary Information: The online version contains supplementary material available at https://doi.org/10.1007/s12039-021-01964-9.

Published online: 09 September 2021

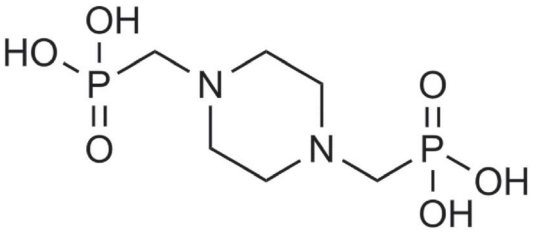

Figure 1. N,N'–piperazine bismethylphosphonic acid linker used in synthesize MIL–91 (Al).

(BET) surface area and pore volume of the material was estimated from N_2 isotherm at 77 K using a Quantachrome Autosorb–IQ–MP/XR instrument. Prior to the nitrogen physisorption experiments, MIL–91(Al) was activated at 443 K for 3 h under helium flow. The specific surface area and pore volumes were calculated by BET model and Barrett–Joyner–Halenda (BJH) method at a relative pressure (P/P_0) of 0.05–0.2 and 0.99, respectively. Thermogravimetric analysis (TGA) was performed 300 K to 900 K with a heating rate of 5 K min^{-1} on a thermogravimetric analyzer (Make: Netzsch, Model: STA449F3A00) under a flow of argon. Powder X-ray diffraction (PXRD) analysis was carried out on Bruker D8 advance instrument operating at 40 kV and 40 mA using Cu Kα (λ = 1.5406 Å) radiation.

2.2 *Pure gas adsorption measurements*

Adsorption equilibria measurements were performed gravimetrically in a Rubotherm magnetic suspension balance. The probe gases (CO_2, CO, N_2, CH_4, C_2H_6 and C_3H_8) were selected due to their relevance in industrially important applications. In addition, they were also selected due to the differences in their polarity and polarizability and molecular size. This will allow us to understand the role of these properties on adsorption in MOFs with small pores such as the one used in this study. The single gas adsorption equilibrium measurements were done gravimetrically at three different temperatures 294, 318 and 358 K over a wide range of pressures. Prior to each isotherm measurement, the adsorbent was activated at 443 K for 3 h under vacuum (about 20 cm^3 min^{-1} purge flow of helium). After activation, data points on each isotherm were collected by the incremental increase in pressure. Equilibrium was ensured before charging to the next higher pressure. All isotherms are reported in terms of excess adsorption quantities calculated from raw measurements using buoyancy corrections. The impenetrable solid volume of adsorbent for buoyancy correction was obtained from helium measurements at 294 K in the pressure range of 0–25 bar, using non adsorbing helium assumption. Fugacity was used instead of pressure to account for non–ideality in the gas phase.[14]

3. Results and Discussion

A Thermogram of MIL–91(Al) was performed on a thermogravimetric analyzer and showed high thermal stability (Figure 2). The weight loss below 430 K, corresponding to the loss of water molecules from the framework channels. The weight loss between 490 and 530 K is analogous to other porous aluminum phosphonates with Al–OH–Al chains, and is likely due to dihydroxylation and subsequent loss of water. The organic ligand breaks down starts at about 630 K. The powder XRD pattern (Figure 3) was similar to earlier reports in the literature.[13] The N_2 adsorption isotherm at 77 K was shown in Figure 4. The sample was activated prior to physisorption measurement at 443 K under vacuum. The calculated surface area and pore volume were 257 m^2 g^{-1} and 0.195 cm^3 g^{-1}, respectively.

3.1 *Adsorption isotherms*

The adsorption isotherms of MIL–91(Al) were evaluated gravimetrically at three different temperatures 294, 318, 358 K with CO_2, CO, N_2, CH_4, C_2H_6 and C_3H_8. Each measurement starts with zero bar pressure and goes to the incremental pressure increase. Every measurement was waited to reach equilibrium and the next pressure was charged.

The isotherms for CO_2, CH_4, CO and N_2 at 294 K are shown in Figure 5. Isotherms at other temperatures are included in Figures S1–S4, SI. At 294 K, the adsorbed amount for CO_2 at 1 bar was 3.0 mol kg^{-1}

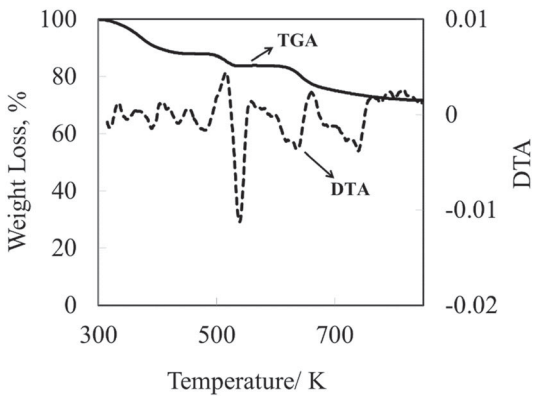

Figure 2. TGA and DTA analysis of MIL–91(Al) at heating rate of 5 K min^{-1} under argon flow.

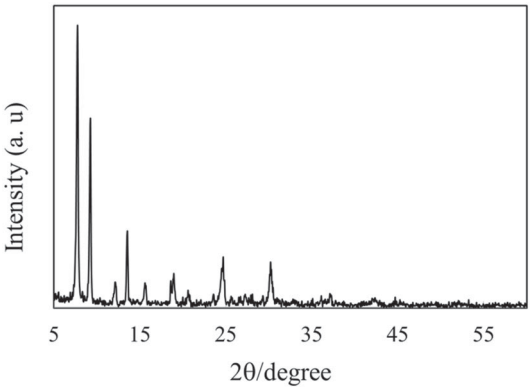

Figure 3. Powder X–ray diffractogram of MIL–91(Al).

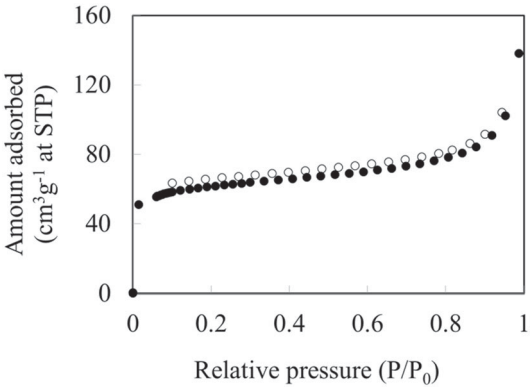

Figure 4.. N_2 adsorption (●) and desorption (○) isotherm of MIL–91(Al) at 77 K.

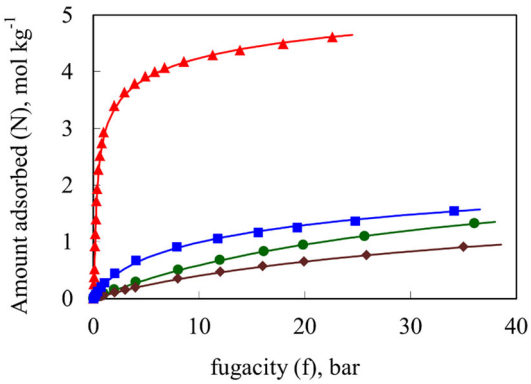

Figure 5. Adsorption Isotherms of CO_2 (▲), CH_4 (■), CO (●) and N_2 (◆) at 294 K. Symbols are experimental data; lines are fits obtained using virial isotherm parameters from Table S2.

and while at 10 bar it was 4.3 mol kg^{-1}. These values are higher compared to other small pores MOFs such as MIL–53(Al)–NH_2 (1.6 mol kg^{-1} at 283 K and 1 bar),[15] Sc–BDC–NO_2 (1.1 mol kg^{-1} at 303 K and 1 bar)[16] and UiO–66(Zr)–$(COOH)_2$ (1.0 mol kg^{-1} at 303 K and 1 bar).[17] However, these uptakes are quite lower compared to Zn–DOBDC (4.6 mol kg^{-1}),[18] Cu–BTC (5.8 mol kg^{-1}).[19] The adsorption capacities of CO and N_2 at 1 bar were found to be 0.08 mol kg^{-1} and 0.06 mol kg^{-1}, respectively. Compared to the CO_2 adsorption uptake, the CO and N_2 uptakes are relatively lower due to lack of strong adsorption sites; CO_2 on the other hand binds strongly to P–OH and N–H sites of the ligand. The uptakes of CO and N_2 at (about 35 bar) was found to be 1.3 mol kg^{-1} and 0.9 mol kg^{-1} respectively, comparable to that on MIL–91(Ti) and Ni–STA–12[12] MOFs. Nevertheless, these adsorbed amounts are relatively low compared to other MOFs with larger pore volumes such as MIL–53(Al)–NH_2,[15] MIL–125 (Ti),[12] MIL–101(Cr),[19] etc.

The saturation adsorption capacities of lower alkanes such as CH_4, C_2H_6 and C_3H_8 are 1.7 (40 bar), 1.1 mmolg^{-1} (10 bar) and 0.8 mmolg^{-1} (2 bar) respectively at 294 K (Figure 6). As expected, adsorption at low pressure increases with an increase in carbon chain length with respect to increase of polarizability and saturation adsorption capacity decreases with the increase of carbon chain length of the alkane due to an increase of molecular size. The uptake capacities of CH_4 and C_2H_6 were lower than Cu–BTC,[19,21] Mg–DOBDC,[20] Zn–DABCO[21] and it is comparable to activated carbon,[22] zeolite 5A,[22] silica gel KC[23] and higher than STH–2GCB.[23] For C_3H_8, loading at 294 K, 0.1 bar is lower than silica gel KC,[22] silicalite, Zn–DABCO,[21] Cu–BTC.[19]

3.2 *Isotherm modeling*

The adsorption isotherms were modeled to get an insight of adsorption. While the accuracy of the models generally depends upon the independent parameters present in the equation. For all gases of experimental data was fitted by Virial model with

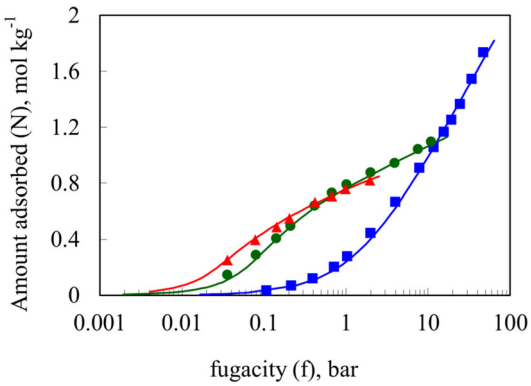

Figure 6. Adsorption Isotherms of CH_4 (■), C_2H_6 (●) and C_3H_8 (▲) at 294 K. Symbols are experimental data; lines are fits obtained using virial isotherm parameters from Table S2, SI.

good statistical significance. The model equation used for the fit was

$$\ln\left(\frac{f}{N}\right) = bN + cN^2 - \ln(\beta) \quad (1)$$

Where b and c are second and third virial coefficients for adsorption. The temperature dependency for these parameters is

$$b = b^{(0)} + \frac{b^{(1)}}{T} \quad (2)$$

$$c = c^{(0)} + \frac{c^{(1)}}{T} \quad (3)$$

The temperature dependency of Henry's constant, β (mol kg^{-1} bar^{-1}) is expressed

$$\beta = \beta^{(0)}\exp\left(\beta^{(1)}/T\right) \quad (4)$$

Where T is temperature in K. The two parameters $\beta^{(0)}$ and $\beta^{(1)}$ are related to entropy and enthalpy of adsorption at zero loading, respectively. The enthalpy of adsorption was calculated by using

$$\Delta h_{ads} = -R\frac{\partial(\ln f)}{\partial(1/T)}\bigg|_N = -R(\beta^{(1)} - b^{(1)}N - c^{(1)}N^2 \quad (5)$$

Where R is the gas constant in J $mol^{-1}K^{-1}$.

The enthalpy of adsorption for CO_2 (−37.5 kJ/mol) is amongst the highest for MOFs without open metal sites. On the other hand, the enthalpy of adsorption for CO and N_2 are −14.7 and −11.9 kJ/mol, respectively; the polarity of these molecules does not play any significant role in the interactions and only dispersion interactions with the surface govern the adsorption process. On the other hand, CH_4 has higher polarizability (even though it is non–polar) resulting in slightly higher adsorption enthalpy. As the carbon chain length increases in C_2H_6 and C_3H_8, their adsorption enthalpies are higher than that of CH_4 (Figure 7).

3.3 *Prediction of binary selectivity using IAST*

In order to evaluate the potential applications of MIL–91(Al), binary gas adsorption was performed from single gas adsorption data using Ideal Adsorbed Solution Theory (IAST). Selectivity for industrially relevant gas mixtures at 294 K and 1 bar is shown in Figure 8.

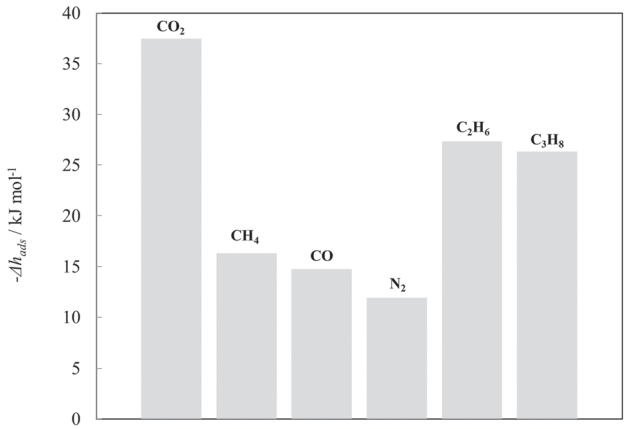

Figure 7. Enthalpy of adsorption at zero coverage of CO_2, CH_4, CO, N_2, C_2H_6 and C_3H_8.

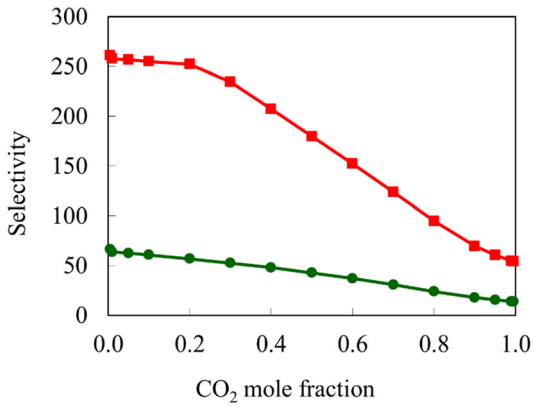

Figure 8. Variation of CO_2 selectivity over N_2 (■) and CH_4 (●) at 294 K and 1 bar; lines are drawn as a guide to the eyes.

For CO_2/N_2 (0.15/0.85), the predicted selectivity is 253 comparatively higher than Cu–BTC, MIL–100(Fe), MIL–101(Cr), MIL–125(Ti)–NH_2 and MIL–47(V).[12] However, it is lower than MIL–53(Al)–NH_2.[12] For CO_2/CH_4 (0.5/0.5), simulated selectivity is 43 comparatively higher than MIL–100 (Fe), MIL–101 (Cr), MIL–125(Ti) and MIL–125(Ti)–NH_2 and lower than MIL–91(Ti)–HT and NaX.[12] The results seem to suggest that small pores with no open metal sites can also be used for selective adsorption of CO_2 with an appropriate choice of ligands.

4. Conclusions

This work reports adsorption of CO_2, CO, CH_4, N_2, C_2H_6 and C_3H_8 were carried out over a wide range of pressures and three different temperatures on MIL–91 (Al). For all adsorbates Type–I isotherm were observed. CO_2 exhibits good adsorption capacity due to its size and interactions with functional groups on

the ligand. For lower alkanes such as CH_4, C_2H_6 and C_3H_8, adsorption at low pressure increases with an increase in carbon chain length; with respect to an increase of polarizability and saturation, adsorption capacity decreases with the increase of carbon number of the alkane due to an increase of molecular size. Although MIL–91(Al) offers excellent selectivity for CO_2, its adsorption enthalpy is only moderate (−37.5 kJ/mol) thereby making it possible for easy regeneration in PSA applications. The small pore size along with the absence of open metal sites and suitable functional groups in the ligand makes this MOF attractive for CO_2 separation applications.

Supplementary Information (SI)

Figures S1-S10 and Tables S1-S2 are available at www.ias.ac.in/chemsci.

Acknowledgements

CVS is grateful to the Department of Science and Technology (SERB), India, (grant codeCRG/2019/000387) for financial aid.

References

1. Li H, Eddaoudi M, O'Keeffe M and Yaghi O M 1999 Design and synthesis of an exceptionally Stable and highly Porous metal–organic framework *Nature* **402** 276
2. Yaghi O M, O'Keeffe M, Ockwig N W, Chae H K, Eddaoudi M and Kim J 2003 Reticular synthesis and the design of new materials *Nature* **423** 705
3. Eddaoudi M, Kim J, Rosi N, Vodak D, Wachter J, O'Keeffe M and Yaghi O M 2002 Systematic design of pore size and functionality in isoreticular MOFs and their application in methane storage *Science* **295** 469
4. Yaghi O M, Li H, Davis C, Richardson D and Groy T L 1998 Synthetic strategies, structure patterns, and emerging properties in the chemistry of modular porous solids *Acc. Chem. Res.* **31** 474
5. Rosi N L, Eckert J, Eddaoudi M, Vodak D T, Kim J, O'Keeffe M and Yaghi O M 2003 Hydrogen storage in microporous metal–organic frameworks *Science* **300** 1127
6. Chen B, Eddaoudi M, Hyde S T, O'Keeffe M and Yaghi O M 2001 Interwoven metal–organic framework on a periodic minimal surface with extra–large pores *Science* **291** 1021
7. Eddaoudi M, Moler D B, Li H, Chen B, Reineke T M, O'Keeffe M and Yaghi O M 2001 Modular chemistry: Secondary building units as a basis for the design of highly porous and robust metal–organic carboxylate frameworks *Acc. Chem. Res.* **34** 319
8. Eddaoudi M, Li H and Yaghi O M 2000 Highly porous and stable metal–organic frameworks: Structure design and sorption properties *J. Am. Chem. Soc.* **122** 1391
9. Fletcher A J, Thomas K M and Rosseinsky M J 2005 Flexibility in metal–organic framework materials: Impact on sorption properties *J. Solid State Chem.* **178** 2491
10. Karra J R and Walton K S 2008 Effect of open metal sites on adsorption of polar and nonpolar molecules in metal–organic framework Cu–BTC *Langmuir* **24** 8620
11. Wang Z and Cohen S M 2009 Postsynthetic modification of metal–organic frameworks *Chem. Soc. Rev.* **38** 1315
12. Benoit V, Pillai R S, Orsi A, Normand P, Jobic H, Nouar F, et al. 2016 MIL–91(Ti), a small pore metal–organic framework which fulfils several criteria: An upscaled green synthesis, excellent water stability, high CO_2 selectivity and fast CO_2 transport *J. Mater. Chem. A* **4** 1383
13. Serre C, Groves J A, Lightfoot P, Slawin A M Z, Wright P A, Stock N, et al. 2006 Synthesis, structure and properties of related microporous N, N′–piperazinebis-methylenephosphonates of aluminum and titanium *Chem. Mater.* **18** 1451
14. Talu O 1998 Needs, status, techniques and problems with binary gas adsorption experiments *Adv. Colloid Interface Sci.* **76–77** 227
15. Stavitski E, Pidko E A, Couck S, Remy T, Hensen E J M, Weckhuysen B M, et al. 2011 Complexity behind CO_2 capture on NH_2–MIL–53(Al) *Langmuir* **27** 3970
16. Pillai R S, Benoit V, Orsi A, Llewellyn P L, Wright P A and Maurin G 2015 Highly selective CO_2 capture by small Pore scandium–based metal–organic frameworks *J. Phys. Chem. C* **119** 23592
17. Yang Q, Vaesen S, Ragon F, Wiersum A D, Wu D, Lago A, et al. 2013 A water stable metal–organic framework with optimal features for CO_2 capture *Angew. Chemie - Int. Ed.* **52** 10316
18. Millward A R and Yaghi O M 2005 Metal–organic frameworks with exceptionally high capacity for storage of carbon dioxide at room temperature *J. Am. Chem. Soc.* **127** 17998
19. Chowdhury P, Mekala S, Dreisbach F and Gumma S 2012 Adsorption of CO, CO_2 and CH_4 on Cu–BTC and MIL–101 metal organic frameworks: Effect of open metal sites and adsorbate polarity *Micropor. Mesopor. Mater.* **152** 246
20. Bao Z, Alnemrat S, Yu L, Vasiliev I, Ren Q, Lu X and Deng S 2011 Adsorption of ethane, ethylene, propane, and propylene on a magnesium–based metal–organic framework *Langmuir* **27** 13554
21. Mishra P, Uppara H P, Mandal B and Gumma S 2012 Adsorption of lower alkanes on a zinc based metal organic framework *J. Chem. Eng. Data* **57** 2610
22. Herden H, Löffler U and Schöllner R 1991 Adsorption of hydrocarbons on activated carbons *J. Colloid Interface Sci.* **144** 477
23. Olivier M G and Jadot R 1997 Adsorption of light hydrocarbons and carbon dioxide on silica gel *J. Chem. Eng. Data* **42** 230